Inorg. Chem. **2005**, *44*, 1672–1685

Syntheses and Characterization of the MF_6^- (M = As, Sb) Salts of the Simple Trithietanylium $PhCS_3^+$ Cation and the Identity of $PhCS_3Cl$

Min Fang, Jack Passmore,* and Andreas Decken

Department of Chemistry, University of New Brunswick, Fredericton, New Brunswick, Canada E3B 6E2

Received February 24, 2004

MF_6^- (M = As or Sb) salts of a simple derivative of the trithietanylium $PhC\overline{SSS}^+$, **1**, were synthesized for the first time by the reaction of $PhCS_3Cl$ and $AgMF_6$ in liquid SO_2. **1**SbF_6 was characterized by IR, FT-Raman, and NMR spectroscopy, elemental analysis, and a preliminary X-ray crystal structure. **1**AsF_6 was characterized by ^1H NMR and FT-Raman spectroscopy. The calculated (MPW1PW91/3-21G* or 6-31G*) geometries, ^1H and ^{13}C chemical shifts (MPW1PW91/6-311G(2DF)//MPW1PW91/3-21G*), and vibrational frequencies and intensities (MPW1PW91/6-31G*) were in satisfactory agreement with the observed values. The calculated π type molecular orbitals of $HC\overline{SSS}^+$ (MPW1PW91/6-311+G*) and **1** (MPW1PW91/3-21G*) imply that the 6π $-C\overline{SSS}^+$ ring has some aromatic character. **1**SbF_6 undergoes a metathesis reaction with NBu_4Cl in liquid SO_2 to give $PhCS_3Cl$, which was characterized by vibrational spectroscopy and mass spectrometry. The evidence indicates that $PhCS_3Cl$ has the ionic formulation $PhC\overline{SSS}^+Cl^-$, with significant cation–anion interactions in the solid state. $ArC\overline{SSS}^+SbF_6^-$ (Ar = 1-naphthyl), **14**SbF_6, was prepared from $ArCS_3Cl$ and $AgSbF_6$, suggesting that the synthesis of MF_6^- (M = As or Sb) salts of $RC\overline{SSS}^+$ is potentially general for aryl derivatives. The structure of **14**SbF_6 was established by ^1H and ^{13}C NMR, IR, and FT-Raman spectroscopy, and theoretical calculations gave values in agreement with the experimental data.

Introduction

The preparation, structure, bonding, chemical reactivities, and corresponding reaction mechanisms of the reactions of small heterocycles have received much attention from both experimental and theoretical perspectives.[1−4] In a previous study, we reported that a 1:1 mixture of $S_4(AsF_6)_2$ and $S_8(AsF_6)_2$ reacted with CH_3CN, producing derivatives of 3,5-dimethyl-1,2,4-thiadiazole and $(C_6H_4N_3S_6^{3+})(AsF_6^-)_3$, **3**$(AsF_6)_3$ (Chart 1),[5] providing the first structural evidence of a trithietanylium heterocycle $-C\overline{SSS}^+$ (referred to as the $-CS_3^+$ ring) and the first structurally characterized example of a $-C\overline{XXX}^+$ (X = O, S, Se, and Te) heterocyclic ring system.[5] However, **3**$(AsF_6)_3$ contained a complex tricyclic trication and was prepared in low yield (<5%).

Isovalent replacement of CR by S^+ in $(CR)_4^{2-}$, **4**, generates the families of related $(CR)_xS_{4-x}$ (x = 0−4) 6π four-membered ring systems as shown in Scheme 1, including the trithietanylium heterocycle $RC\overline{SSS}^+$ cation, **1** (R = Ph), the subject of this report. Cyclobutadiene dianion, **4** (R = $SiMe_3$),[6] 1,2-dithiete, **7** ($R_2C_2S_2$, R = CF_3, CO_2Me, 1-adamantyl),[7−9] and S_4^{2+}, **8**,[10] are known. Although **6** is unknown,

* To whom correspondence should be addressed. E-mail: passmore@unb.ca.

(1) Fowler, J. E.; Galbraith, J. M.; Vacek, G.; Schaefer, H. F., III *J. Am. Chem. Soc.* **1994**, *116*, 9311−9319.
(2) Driess, M.; Grutzmacher, H. *Angew. Chem., Int. Ed.* **1996**, *35*, 829−856.
(3) Harris, P. A. In *Comprehensive Heterocyclic Chemistry II*; Katritzky, A. R., Rees, C. W., Scriven, E. F. V., Eds.; Pergamon: New York, 1996.
(4) Zoller, U. In *Comprehensive Heterocyclic Chemistry II*; Katritzky, A. R., Rees, C. W., Scriven, E. F. V., Eds.; Pergamon: New York, 1996.
(5) Cameron, T. S.; Decken, A.; Fang, M.; Parsons, S.; Passmore, J.; Wood, D. J. *Chem. Commun.* **1999**, 1801−1802.
(6) Sekiguchi, A.; Matsuo, T.; Watanabe, H. *J. Am. Chem. Soc.* **2000**, *122*, 5652−5653.
(7) Hencher, J. L.; Shen, Q.; Tuck, D. G. *J. Am. Chem. Soc.* **1976**, *98*, 899−902.
(8) Shimizu, T.; Murakami, H.; Kobayashi, Y.; Iwata, K.; Kamigata, N. *J. Org. Chem.* **1998**, *63*, 8192−8199.
(9) Donahue, J. P.; Holm, R. H. *Acta Crystallogr., Sect. C* **1998**, *54*, 1175−1178.

10.1021/ic049759s CCC: $30.25
Published on Web 02/18/2005

Chart 1. Structure Legend

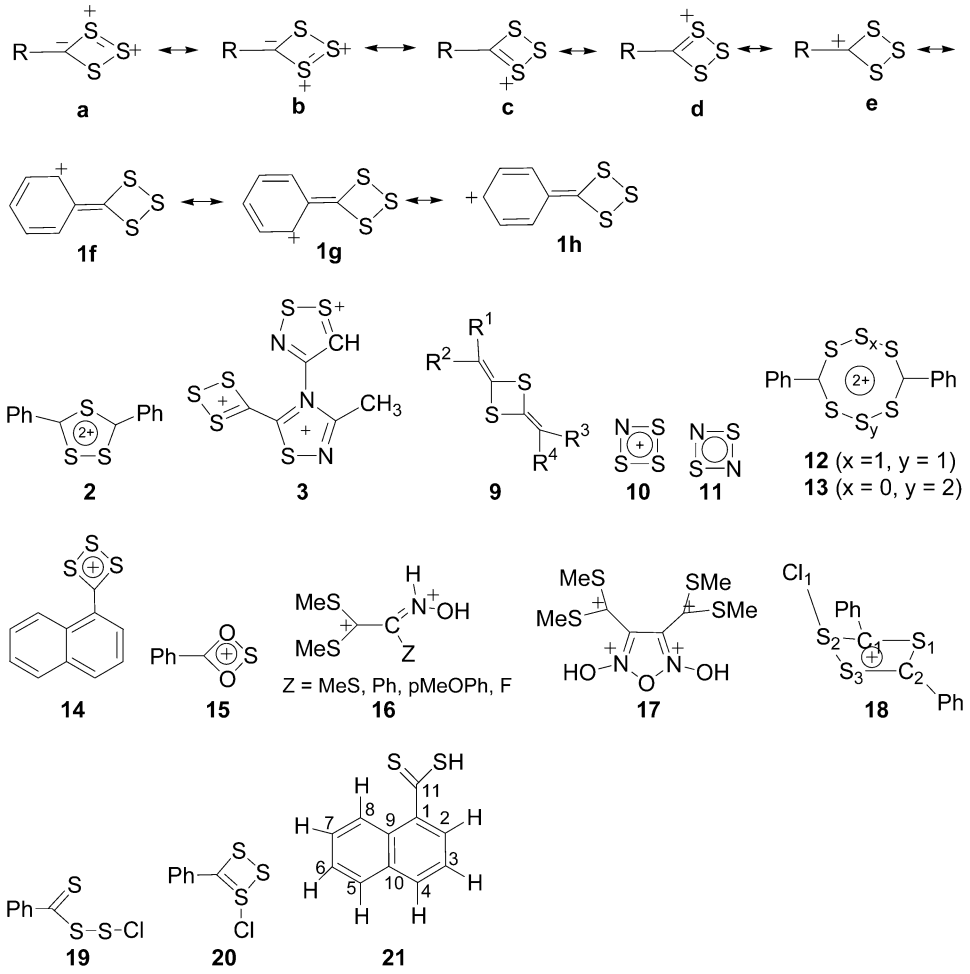

Scheme 1 The 6π Four-Membered Ring Series Formed by the Replacement of CR by S^+ in $(RC)_4^{2-}$ (**4**)

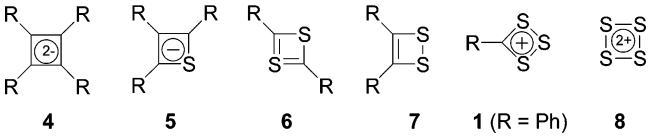

the related **9** (Chart 1) has been characterized.[11−13] The $-CS_3^+$ ring is also isoelectronic to the unknown S_3N^+, **10** (Chart 1), although the isolobal ring S_2N_2, **11**, is well characterized.[14−16] Recently, a compound containing the related 6π aromatic ring P_4^{2-} has also been reported.[17] Zahradnik[18] predicted from molecular orbital calculations in 1965 that RCS_3^+ was very unlikely to be stable due to steric strain and high energy. However, Campaine et al. showed[19] that the reaction of arenedithioic acids ($ArCS_2H$, Ar = Ph, *p*-$MeOC_6H_4$, and 1-naphthyl) with SCl_2 according to eq 1 resulted in the formation of yellow compounds with the empirical formulas $ArCS_3Cl$. They were tentatively identified as 4-aryltrithietanylium chlorides, although the authors did not exclude the possibility that they might be dimeric or polymeric.

$$ArCS_2H + SCl_2 \rightarrow ArCS_3Cl + HCl \qquad (1)$$
$$Ar = Ph,\ 4\text{-}MeOC_6H_4,\ 1\text{-naphthyl}$$

In this paper, we report the preparation, by the reaction of $PhCS_3Cl$ and $AgMF_6$ in liquid SO_2, of **1**MF_6 (M = As or Sb) containing the simple phenyl derivative of the trithietanylium ring and characterization by spectroscopic methods as well as a preliminary X-ray crystal structure of **1**SbF_6. The oxidation of $Zn(PhCS_2)_2$ by AsF_5 in liquid SO_2 also produced **1**AsF_6 (^{1}H NMR). **1**SbF_6 converted to **2**$(SbF_6)_2$ in liquid SO_2, a full account of which will be reported elsewhere.[20] $ArCS_3SbF_6$ (Ar = 1-naphthyl), **14**SbF_6 (NMR, IR and FT-Raman), was similarly prepared, implying that

(10) Cameron, T. S.; Dionne, I.; Jenkins, H. D. B.; Parsons, S.; Passmore, J.; Roobottom, H. K. *Inorg. Chem.* **2000**, *39*, 2042−2052 and references therein.
(11) Schweizer, E. E.; Hayes, J. E.; Rheingold, A.; Wei, X. *J. Org. Chem.* **1987**, *52*, 1810−1812.
(12) Rudershausen, S.; Holdt, H.-J.; Reinke, H.; Drexler, H.-J.; Michalik, M.; Teller, J. *Chem. Commun.* **1998**, 1653−1654.
(13) Selzer, T.; Rappoport, Z. *J. Org. Chem.* **1996**, *61*, 7326−7334.
(14) Goehring, M.; Voigt, D. *Naturwissenschaften* **1953**, *40*, 482−482.
(15) Warn, J. R. W.; Chapman, D. *Spectrochim. Acta* **1966**, *22*, 1371.
(16) Mikulski, C. M.; Russo, P. J.; Saran, M. S.; MacDiarmid, A. G.; Garito, A. F.; Heeger, A. J. *J. Am. Chem. Soc.* **1975**, *97*, 6358−6363.
(17) Kraus, F.; Aschenbrenner, J. C.; Korber, N. *Angew. Chem., Int. Ed.* **2003**, *42*, 4030−4033.
(18) Zahradník, R. *Adv. Heterocycl. Chem.* **1965**, *5*, 1−67.
(19) Campaine, E.; Pragnell, M.; Haaf, F. *J. Heterocycl. Chem.* **1968**, *5*, 141−144.
(20) Cameron, T. S.; Decken, A.; Fang, M.; Passmore, J. *Chem. Commun.* **2001**, 1370−1371. A full account of the synthesis and characterization of **2**$(SbF_6)_2$ and the conversion from **1**SbF_6 to **2**$(SbF_6)_2$ is in preparation.

the synthesis of MF_6^- (M = As or Sb) salts of RCS_3^+ is potentially general for aryl derivatives. We present evidence that $PhCS_3Cl$[19] has an ionic $Ph\overline{CSSS}^+Cl^-$ structure with substantial cation−anion interaction. A preliminary account of part of this work has been reported.[20]

Experimental Section

Materials. Regents were from Aldrich unless otherwise specified and used without further purification. $AgSbF_6$ (SynQest Labs. Inc., 99%) and AsF_5 (Ozark Mahoning) were used as received. SO_2 (Liquid Air, 100%) was distilled onto CaH_2 and stored for at least 12 h prior to use. $AgAsF_6$ was prepared by the reaction of Ag and AsF_5 in liquid SO_2.[21] CCl_4 was dried over P_2O_5 and stored over 4 Å molecular sieves. CH_2Cl_2 and diethyl ether (ACP, water 0.03%) were dried over CaH_2 and Na (benzophenone as an indicator), respectively, and distilled before use. CS_2 was dried over CaH_2 for at least 7 days. $Zn(PhCS_2)_2$ was prepared as reported[22,23] and dried under dynamic vacuum to constant weight. Tetrabutylammonium chloride[24] (5−10 g) (NBu_4Cl, Across, 95% tech) was dissolved with a small amount of hot acetone (∼10 mL) (40−50 °C). Once dissolved, a 2−3-fold excess (by volume) of dry diethyl ether was added with precipitation of NBu_4Cl. The precipitate was then quickly filtered and dried under dynamic vacuum, shown to be water free by IR spectroscopy, and then stored in the drybox.

$PhCS_2H$ in diethyl ether was synthesized[22] and purified[25] as reported. The concentration of the acid was determined by back-titration using a pH meter, and the acid was stored at 5 °C and used within 1 week. ^{1}H NMR (400 MHz, $CDCl_3$): δ 6.40 (s, broad, 1H, $-CS_2H$), 7.41 (t, $^2J_{HH}$ = 7.6, 2H, *m*-C_6H_5), 7.59 (t, $^2J_{HH}$ = 7.6 Hz, 1H, *p*-C_6H_5), 8.06 (d, $^2J_{HH}$ = 8.4 Hz, 2H, *o*-C_6H_5). SCl_2 was synthesized as reported[26] and purified by double distillation under reduced pressure (200−300 mmHg). The purified SCl_2 was collected in a Schlenk vessel containing 1−2% PCl_5 (stabilizer) and used within 1 week.[26]

General Procedures. General apparatus and techniques, unless specified, have previously been described.[27,28] All reactions using Ag^+ salts were carried out in the dark. Reactions using SO_2 as solvent were carried out in a two-bulb−two-valve Pyrex glass vessel incorporated with a medium sintered glass frit unless specified otherwise (panel B in S-Figure 1).

Samples for ^{1}H, ^{13}C {^{1}H}, and ^{19}F NMR spectroscopy were contained in sealed 5 or 10 mm thick-walled NMR tubes. NMR spectra were obtained unlocked at 298 K on a Varian Unity 400 spectrometer. Spectra were referenced externally to a solution of TMS in liquid SO_2 (^{1}H and ^{13}C) or $CFCl_3$ in liquid SO_2 (^{19}F).

FT-IR spectra of KBr pellets of samples (for $PhCS_3Cl$) or neat fine powders between KBr plates (for **1**SbF_6) were recorded at 293 K in the range of 4000−400 cm^{-1} on a Bruker IFS66 FT-IR spectrometer. FT-Raman spectra were recorded at 293 K on a Bruker IFS66 FT-IR equipped with a Bruker FRA106 FT-Raman accessory using a Nd:YAG laser (emission wavelength, 1064 nm; maximum laser power, 3009 mW). Samples were sealed in melting point capillaries, and data were collected in the backscattering mode (180 excitation; resolution, 2.0 or 4.0 cm^{-1}).

Chemical analyses were carried out by Galbraith Laboratories, Inc. (Knoxville, TN).

Samples were sealed in glass capillaries under dry nitrogen and introduced into the mass spectrometer via the direct inlet. All spectra (low resolution) were obtained at room temperature in an electron impact mode using 27 eV ionization voltage on a Kratos MS-50TC instrument.

X-ray powder diffraction patterns were recorded using a Rigaku Miniflex diffractometer with Cu Kα radiation. Samples were mounted with petroleum jelly (Vasoline) on a single-crystal silicon wafer. A $\theta-2\theta$ goniometer was used to obtain the diffraction angles in the region 5−90° at a rate of 1°/min.

Theoretical calculations were carried out using Gaussian 98W.[29] Geometry optimizations were performed at the MPW1PW91[30] level with 3-21G* or 6-31G* basis sets. All optimized geometries were stationary points, and energies included zero-point energies. Visualizations of optimized structures were made using Schwenk's RESVIEW program,[31] and graphic representations of calculated molecular orbitals were obtained using Chem3D.[32] The vibrational spectra were calculated at the MPW1PW91/6-31G* level based on the optimized geometry (MPW1PW91/6-31G*). Calculated vibrational modes were animated and assigned using Hyperchem.[33] Natural bond orbital (NBO) analyses were performed at the MPW1PW91/6-31G* level using the NBO package integrated in G98W. Isotropic NMR shielding tensors were calculated at the MPW1PW91/6-311G(2DF) level based on the optimized geometry (MPW1PW91/3-21G*) and referenced against the calculated TMS values.

Synthesis of $PhCS_3Cl$. $PhCS_3Cl$ was prepared as reported with some modifications.[19] In a typical reaction, $PhCS_2H$ (4.8 mmol) in dry diethyl ether (50 mL) was added (2−5 min) with stirring to SCl_2 (0.81 g, 7.9 mmol) in dry diethyl ether (15 mL). The yellow solid ($PhCS_3Cl$, mp 90−93 °C) which immediately precipitated was collected on filtration under nitrogen and dried under a dynamic vacuum. Yield: 0.412 g, 1.86 mmol, 38.8% (based on $PhCS_2H$). Other synthetic data are included in the Supporting Information (S-Table 1).[34] The FT-Raman spectrum of $PhCS_3Cl$ in the region 1650−50 cm^{-1} region is given in Figure 1, the full range FT-Raman (4000−50 cm^{-1}) and FT-IR spectra (4000−400 cm^{-1}) are shown in S-Figure 2, and tentative assignments are given in Table 1. Mass spectral data of $PhCS_3Cl$ are listed in Table 2.

The soluble product isolated from the filtrate after the removal of the solvent (S-Table 1) was usually a yellow powder mixed with a red glassy solid, which was attentively identified as mainly

(21) Roesky, H. W.; Witt, M. *Inorg. Synth.* **1986**, *24*, 72−76.
(22) Houben, J. *Chem. Ber.* **1906**, *39*, 3219−3224.
(23) Luciani, M. L.; Furlani, C. *Inorg. Chem.* **1968**, *8*, 1586−1592.
(24) Rawson, J. M. University of Cambridge, Cambridge, personal communication.
(25) Bost, R. W.; Shealy, O. L. *J. Am. Chem. Soc.* **1951**, *73*, 25−28.
(26) Rosser, R. J.; Whitt, F. R. *J. Appl. Chem.* **1960**, *10*, 229−237.
(27) Murchie, M. P.; Kapoor, R.; Passmore, J.; Schatte, G.; Way, T. *Inorg. Synth.* **1997**, *31*, 102−112.
(28) Brownridge, S.; Cameron, T. S.; Passmore, J.; Schatte, G.; Way, T. C. *J. Chem. Soc., Dalton Trans.* **1996**, 2553−2570.
(29) Frisch, M. J.; Trucks, G. W.; Schlegel, H. B.; Gill, P. M. W.; Johnson, B. G.; Robb, M. A.; Cheeseman, M. A.; Keith, T.; Petersson, G. A.; Montgomery, J. A.; Raghavachari, K.; Al-Laham, M. A.; Zakrzewski, V. G.; Ortiz, J. V.; Foresman, J. B.; Cioslowski, J.; Stefanov, B. B.; Nanayakkara, A.; Challacombe, M.; Peng, C. Y.; Ayala, P. Y.; Chen, W.; Wong, M. W.; Andres, J. L.; Replogle, E. S.; Gomperts, R.; Martin, R. L.; Fox, D. J.; Stratmann, R. E.; Burant, J. C.; Dapprich, S.; Millam, J. M.; Daniel, A. D.; Kudin, K. N.; Strain, M. C.; Farkas, O.; Tomasi, J.; Barone, V.; Cossi, M.; Cammi, R.; Mennucci, B.; Pomelli, C.; Adamo, C.; Clifford, S.; Ochterski, J.; Cui, Q.; Morokuma, K.; Malick, D. K.; Rabuck, K.; Liu, G.; Liashenko, A.; Piskorz, P.; Komaromi, I.; Head-Gordon, M.; Gonzalez, C.; Pople, J. A. *Gaussian 98W*, version 5.2; Gaussian, Inc.: Pittsburgh, PA, 1998.
(30) Adamo, C.; Barone, V. *J. Chem. Phys.* **1998**, *108*, 664−675.
(31) Schwenk, H. *RESVIEW*, version 2.21; 1998.
(32) *Chem 3D Ultra*, version 4.5; CambridgeSoft Corp.: Cambridge, MA, 1998.
(33) *Hyperchem*, version 3.0; Autodesk: San Rafael, CA, 1993.
(34) "S-Figure *X*" (*X* = 1−19) and "S-Table *Y*" (*Y* = 1−7) are included in the Supporting Information.

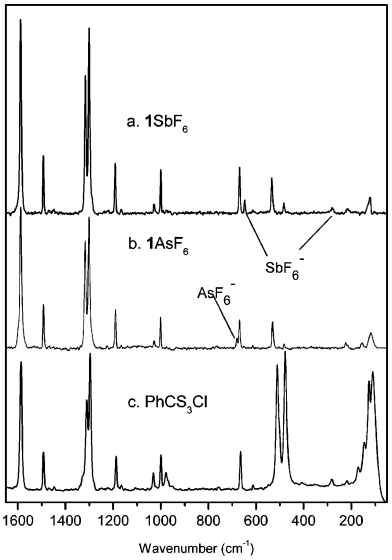

Figure 1. FT-Raman spectra of **1**SbF_6 (trace a, baseline corrected, resolution 2.0, 3000 scans, laser power 2.7 mW), **1**AsF_6 (trace b, baseline corrected, resolution 2.0, 5000 scans, laser power 10 mW), and $PhCS_3Cl$ (trace c, resolution 4 cm^{-1}, 50 scans, laser power 11 mW) in the region 1650−50 cm^{-1}.

$Ph_2C_2S_3Cl_2$, **18**Cl.[20] In several cases when using diethyl ether as a solvent, an unidentified red viscous oil was recovered as the only soluble product (S-Table 1).

Properties of $PhCS_3Cl$. Campaine et al.[19] reported that $PhCS_3Cl$ is insoluble in organic solvents, but we found that it dissolves in CH_2Cl_2 to give a yellow solution that quickly becomes brown and then red-brown, indicating that it is unstable in CH_2Cl_2. Attempts to grow crystals of $PhCS_3Cl$ in liquid SO_2, in which the solubility was low, were unsuccessful;[35] instead $PhCS_3Cl$ gradually turned into a red oil over 12 h.

Synthesis of 1SbF_6. In a typical reaction, an SO_2 solution (about 10 g) of $AgSbF_6$ (0.953 g, 2.77 mmol) in bulb 1 of a three-bulb−three-valve vessel incorporating two medium sintered glass frits (panel A in S-Figure 1) was poured onto $PhCS_3Cl$ (0.570 g, 2.59 mmol) in bulb 2. A yellow solution over a yellow-white solid was formed immediately. After the mixture was stirred for 2 h, the soluble products were extracted into bulb 1, leaving 0.24 g of a red insoluble solid (mainly AgCl, X-ray powder diffraction). The solution in bulb 1 was concentrated to about 2 mL with precipitation of **1**SbF_6 and filtered into bulb 3; the remaining solid was washed by liquid SO_2 (3 × 2 mL). The resulting solution containing the most soluble components (e.g., unreacted $AgSbF_6$ and impurities) was filtered to bulb 3. Bright yellow crystalline **1**SbF_6 (0.492 g, 1.17 mmol, 45.2% based on $PhCS_3Cl$ and eq 1) was obtained in bulb 1 after removing the volatiles under dynamic vacuum. Other synthetic data are included in S-Table 2. The ^1H and ^{13}C NMR chemical shifts of **1**SbF_6 in SO_2 (15 mg in 1.5 g SO_2) are given in Table 3, and the actual spectra are included in the Supporting Information (S-Figure 10 and S-Figure 11). The FT-Raman spectrum in the 1650−50 cm^{-1} region is given in Figure 1, the vibrational frequencies and assignments are given in Table 3, and the full range FT-Raman (4000−50) cm^{-1} and FT-IR spectra (4000−400 cm^{-1}) of **1**SbF_6 are shown in S-Figure 3. The solubility of **1**SbF_6 in liquid SO_2 is about 0.2 g/10 g SO_2 at room temperature. Crystals of **1**SbF_6 were obtained (see Supporting Information), and a preliminary X-ray crystal structure was obtained (triclinic, $P\,\bar{1}$ (no. 2), R1 = 0.103 and wR2 = 0.256, cell parameters: a = 6.899(3) Å, b = 6.905(2) Å, c = 14.651(4) Å, α = 88.78(1)°, β = 88.44(1)°, γ = 60.34(1)°), Z = 12, and V = 606(2) $Å^3$), confirming the atom connectivity. Yellow crystalline **1**SbF_6 (0.346 g) containing a trace of S_8 (FT-Raman) was obtained after further purification (details are given in the Supporting Information). Found (calcd): C, 19.63 (19.90); H, 1.26 (1.20); S, 24.65 (22.80); Sb, 29.39 (28.90), F, 28.63 (27.10)%. All attempts to obtain a mass spectrum of **1**SbF_6 or a spectrum from a mixture of **1**SbF_6 and CsF were unsuccessful. Attempted syntheses of **1**SbF_6 in SO_2Cl_2, CH_2Cl_2, or diethyl ether were unsuccessful.

1AsF_6 was obtained similarly, according to eq 3 using $AgAsF_6$ in an attempt to grow high-quality single crystals for X-ray structure determination. The FT-Raman spectrum of the 1650−50 cm^{-1} region is shown in Figure 1 (no peaks were observed in the region 4000−1650 cm^{-1}), and the frequencies and assignments are given in Table 1.

Attempted Synthesis of $2(AsF_6)_2$ by the Reaction of $Zn(PhCS_2)_2$ and AsF_5 Leading to In Situ Detection of 1AsF_6 in Solution. An in situ room temperature ^1H NMR study of the reaction of AsF_5 (1.33 g, 7.84 mmol) and $Zn(PhCS_2)_2$ (0.436 g, 1.17 mmol) in liquid SO_2 (12.85 g) according to proposed eq 4 was carried out in an attempt to synthesize **2**$(AsF_6)_2$. The ^1H NMR spectrum (in liquid SO_2) (S-Figure 16) showed (after 12 h) **1** (39.4% H), **2** (12.1% H), **12**[20] or **13**[20] (5.0% H), and unidentified compounds (43.5% H). A green precipitate appeared after 7 days, and the ^1H NMR spectrum showed **1** (54% H), **2** (10.0% H), **12** or **13** (6.8% H), and unidentified compounds (29.2% H).

Interconversions of 1SbF_6 and $PhCS_3Cl$. An SO_2 solution of NBu_4Cl (0.103 g, 0.371 mmol in 4 g SO_2) was poured onto an SO_2 (5 g) solution of **1**SbF_6 (0.107 g, 0.254 mmol), resulting in the immediate formation of a yellow solid. The mixture was stirred for 30 s, the solution filtered, and the solvent removed to a constant weight. The FT-Raman spectrum (S-Figure 6) of the precipitated yellow solid (0.021 g, 0.095 mmol) showed only $PhCS_3Cl$.

The yellow solid $PhCS_3Cl$ (0.015 g, 0.068 mmol) from the above reaction was mixed with a solution of excess $AgSbF_6$ (0.121 g, 0.352 mmol) in liquid SO_2 (2.5 g) in a two-bulb−two-valve vessel incorporating a medium sintered glass frit and a 5 mm NMR tube. An aliquot of the solution was filtered into the 5 mm NMR tube after 2 min of stirring, and the tube sealed. The ^1H NMR spectrum (S-Figure 5) recorded after 15 min showed **1** (∼74% H), **2** (5% H), **12** or **13** (6% H), and unidentified compound(s) (∼11% H). The isolated soluble product contained **1**SbF_6 and unreacted $AgSbF_6$ (FT-Raman).

Synthesis of 14Cl. α-Dithionaphthoic acid, $C_{10}H_7CS_2H$, **21**, in dry diethyl ether was obtained in 34.9% yield as described for the synthesis of $PhCS_2H$. ^1H NMR (400 MHz, $CDCl_3$) (shown in S-Figure 4): δ 6.85 (broad s, 1H, SH), 7.47 (t, $^2J_{HH}$ = 7.6, $^3J_{HH}$ = 1.2, 1H, C7−H), 7.53−7.61 (2 td, $^2J_{HH}$ = 6.8−7.2, $^3J_{HH}$ = 1.2−1.6, 2H, C6−H and C3−H), 7.65 (dd, $^2J_{HH}$ = 6.8, $^3J_{HH}$ = 1.2, 1H, C2−H), 7.88−7.93 (2 d, $^2J_{HH}$ = 8.8, $^3J_{HH}$ = 1.6, 2H, C5−H and C8−H), 8.37 (dd, $^2J_{HH}$ = 8.8, $^3J_{HH}$ = 1.6, 1H, C4−H). The ^1H spectrum of $C_{10}H_7CS_2H$ has not hitherto been reported.

14Cl was synthesized (eq 9) as reported in 60−74% yield.[19] The FT-IR (4000−400 cm^{-1}) and FT-Raman spectra (4000−50 cm^{-1}) of **14**Cl (mp: 90−91 °C) are shown in S-Figure 7, and the

(35) $PhCS_3Cl$ is probably reduced by SO_2 according to the following equations, similar to the reduction of $S_3N_2Cl_2$ to $(S_3N_2Cl)_2$ by SO_2 (ref 65).

$$2\ PhCS_3Cl\ +\ SO_2 \rightarrow 2\ PhCS_3^{\bullet}\ +\ SO_2Cl_2$$

$$2\ PhCS_3^{\bullet} \rightarrow (PhCS_3)_2 \rightarrow PhC(S)S\ -\ S(S)CPh\ +\ 1/4\ S_8$$

$$SO_2\ +\ 2\ S_3N_2Cl_2 \rightarrow (S_3N_2Cl)_2\ +\ SO_2Cl_2$$

Table 1. Vibrational Data for $1MF_6$ (M = As, Sb) and $PhCS_3Cl$ Compared with Calculated (MPW1PW91/6-31G*//MPW1PW91/6-31G*) Values for **1** and $PhCS_2^-$ and Those Observed Values for Monosubstituent Benzene Derivatives

$1SbF_6$		$1AsF_6$	$PhCS_3Cl$		Calculated values PhX^b for 1[a]			Calculated values $KPhCS_2^c$ for $PhCS_2^-$[a]			$In(PhCS_2)_3^c$		Assignments[e,h]	
IR[d,f]	Raman	Raman	IR[d,g]	Raman	No.	υ (I_{IR}, I_{Ra})	(X = F, Cl, Br, I)	No.	υ (I_{IR}, I_{Ra})	IR[d]	Raman	IR[d]	Raman		
					1	19(0,1)		1	35(0,5)						
				110(10)	2	89(1,1)		2	128(1,6)		115(5)		124(3)		
					3	118(0,0)		3	201(0,1)		155(3)		176(0.5)		
	123(2.2)	118(1.9)		126(1.0)											
				146(2.3), 171(0.8)											
		156(0.3)		219(0.1)	4	175(1,2)	167-242	5	332(6,2)	330 m	327(0.2)	321 m	330(0.1)	ω_{30}	
	216(0.3)	222(0.5)		282(0.2)	5	272(2,16)		4	270(6,2)						δ(two rings)
					6	344(0,1)	220-368							ω_{24}	δ(two rings)
	280(0.4)														$\upsilon_5(SbF_6^-)$
												360 m,sh			$\upsilon_{asym}MS_2^c$
					7	370(0,0)	398-405	6	402(0,3)					ω_{14}	δ(phenyl ring)
					8	391(2,1)		8	449(3,1)	435 w, b		429 w, b			δ(phenyl ring) out of plane+δ(SCS) out of plane (*not assigned*)[c]
	483(0.3)	482(0.1)	479 w	477(4.9)	9	469(0,14)		7	424(0,12)	490 m	435(7)	462 w	461(7)		**$\delta_{sym}(CS_3$ ring) or $\delta(CS_2)$ in $PhCS_2^-$**
	534(1.6)	531(1.5)	502 w	498(0.7)	10	515(0,16)									**υ_{asym}(SSS)**
				511(4.1)	11	515(14,21)									**CS_3 ring breathing+υ_{sym}(SSS)**
			549 w		12	546(0,1)		9	579(3,4)	598 m		590 m		ω_{29}	δ(phenyl ring) out of plane+δ(SCS) out of plane
							450-496							ω_{29}	
	614(0.1)	614(0.1)		613(0.1)	13	593(1,8)	611-615	10	605(1,5)	621 w	619(0,8)	617 w	612(2)	ω_{23}	δ_{asym}(phenyl ring)
	648(0.6)														$\upsilon_1(SbF_6^-)$
649 m															$\upsilon_3(SbF_6^-)$
660 m			672 s	665(0.7)	14	648(39,28)	656-806	11	643(13,10)	658 m	657(6)	656 s	656(8)	ω_{10}	δ_{sym}(phenyl ring)
677 m	669(1.8)	669(1.3)	672 s		15	649(38,1)	683-684	12	675(25,3)	699 vs		677 s, sh; 680 vs		ω_{28}	δCH out of plane
		680(0.5)													$\upsilon_1(AsF_6^-)$
767 s			753 s	756(0.1)	16	757(44,0)	730-755	13	747(35,0)	769 vs	772(0.3)	765 vs	765(1)	ω_{27}	δCH out of plane
			838 w		17	803(1,4)	831-838	14	821(2,6)	842 w, 853 w	842(0.5)	830 w, b	833(0.5), 846(0.8)	ω_{13}	δCH out of plane.
			875 w, 912 w		18	919(1,1)	894-906	16	890(7,2)					ω_{26}	δCH out of plane
962 m	962(0.1)		975 w	977(0.5)	19	946(15,2)		15	887(39,16)	910 s, 926 m	910(3)	918 s, 924 s, 933 m, sh	918(1), 926(0.8)	ω_{11}	**phenyl ring breathing+υ_{sym}(SCS)** *(926 m and 933 m,sh were assigned to ω_{26})*[c]
							268-517							ω_{11}	
					20	957(0,1)	955-963	17	937(6,1)					ω_{12}	δCH out of plane
	1000(1.4)	1001(1.1)		1000(0.6)	21	971(8,41)	997-1010	19	977(1,34)	1005 m, sh	1002(9)		1001(7)	ω_9	phenyl ring breathing
999 m			999 m		22	989(29,0)		20	1014(261,11)	1020 vs, b	1018(1),b	985 vs, sh; 990 vs, 1000 vs	988(0.8), 993 (1)		**υ_{asym}(SCS)**
					23	997(1,1)	1017-1020	18	945(2,2)					ω_{25}	δCH out of plane
	1028(0.4)	1028(0.3)	1044 m	1031(0.3)	24	1019(3,45)	979-988	21	1023(8,29)			1022 m, sh	1020(2)	ω_8	δ_{asym}CH/δ(phenyl ring)
			1079 m												?
			1103 m		25	1102(2,1)	1061-1065	22	1076(44,7)	1077 m, 1084 s		1100 w		ω_{22}	δCH
	1166(0.2)	1166(0.1)		1167(0.1)	26	1162(0,12)	1156-1160	23	1134(0,12)	1145 w, b	1150(1)	1161 m	1162(0.8)	ω_{21}	δCH

Table 1 (Continued)

$1SbF_6$		$1AsF_6$	$PhCS_3Cl$		Calculated values PhX^b for 1[a]			Calculated values $KPhCS_2^c$ for $PhCS_2^-$[a]				$In(PhCS_2)_3^c$		Assignments[e,h]	
IR[d,f]	Raman	Raman	IR[d,g]	Raman	No.	υ (I_{IR}, I_{Ra})	(X = F, Cl, Br, I)	No.	υ (I_{IR}, I_{Ra})	IR[d]	Raman	IR[d]	Raman		
1193 m	1192(1.8)	1190(1.8)	1186 m, 1203 m	1188(0.6)	27	1181(35,28)	1122-1179	24	1145(30,58)	1170 m	1165(3)	1180 s	1173(2), 1177(2), 1187(6)	ω_7	δ_{sym}CH
					28	1309(6,0)	1255-1295	26	1277(9,0)	1285 w, sh 1305 m		1312 m		ω_{20}	υ_{asym}(C-C in Ph) (ω_{17})[c]
1301 s, 1318 s	1301(10), 1317(6.6)	1301(8.7), 1317(6.6)	1294 s, 1311 s	1296(3.2), 1311(3.0)	29	1332(482,335)	1062-1222	25	1175(12,148)	1212 s	1212(10)	1220 vs, 1236 vs	1220(10), 1234(4)	ω_6	υ_{sym}(Ph-C)
			1338 s		30	1350(7,11)	1321-1326	27	1323(1,0)	1340 vw, b		1332 w,b		ω_{17}	δCH in plane (ω_{20})[c]
			1384 m							1390 w		1380 w,b			?
1449 s	1450(0.2)		1444 s	1448(0.1)	31	1440(31,13)	1436-1462	28	1430(13,4)	1438 s		1444 m	1448(0.8)	ω_{19}	δ_{sym}CH in plane/υ(C-C in Ph)
	1493(1.8)	1492(1.8)		1493(0.7)	32	1482(42,28)	1474-1495	29	1469(11,23)	1470 m		1477 m	1482(4)	ω_5	δ_{sym}CH in plane/υ(C-C in Ph)
					33	1568(1,1)	1573-1601	30	1582(0,0)	1570 vw		1575 w		ω_{18}	υ(C=C)/δCH (ω_4)[c]
1588 s	1589(9.8)	1588(10.0)	1588 m	1587(3.5)	34	1597(177,401)	1573-1598	31	1601(5,161)	1585 m	1582(6)	1589 m	1590(9)	ω_4	υ(C=C)/δ_{sym}CH (ω_{18})[c]
					35	3078(1,27)	3030-3080	35	3098(11,1)					ω_{16}	υ_{asym}CH
					36	3078(0,16)	3030-3080	36	3099(12,140)					ω_2	υ_{sym}CH
					37	3110(0,82)	3030-3080	32	3045(0,69)					ω_3	υ_{asym}CH
				3049(0.4)	38	3122(0,112)	3030-3080	33	3057(53,128)					ω_{15}	υ_{asym}CH
				3071(0.3)	39	3127(0,320)	3030-3080	34	3073(74,234)					ω_1	υ_{sym}CH

[a] The calculated frequencies of **1** and $PhCS_2^-$ scaled by a factor of 0.957 with IR and Raman intensities in parentheses (IR intensities (km·mol^{-1}) and Raman intensities (Å^4·amu^{-1})). [b] Data and assignments from ref 50. [c] Vibrational data and assignments from ref 52. Some assignments have been revised (original assignments given in italics and parentheses) based on the calculated results for $PhCS_2^-$. Depictions of the calculated vibrational modes for $PhCS_2^-$ are given in S-Figure 19. [d] vs = very strong; s = strong; ms = medium strong; m = medium; w = weak; vw = very weak; b = broad. [e] Assignments for $PhCS_3^+$ in $\mathbf{1}MF_6$ and $PhCS_3Cl$ were made based on visualisation of calculated vibrational modes of **1** (S-Figure 14) using Hyperchem,[33] and therefore subject to interpretation, sometimes non trivial for the more complex vibrations. Symbols of ω_x (x = 1 to 30) were used by Schmid, et al.[50] to represent the monosubstituted phenyl ring vibrations, among which ω_6, ω_{10}, ω_{11}, ω_{24},ω_{29}, ω_{30} (in bold) are substituent sensitive. A plus sign indicates two vibrations of roughly equal intensity; a solidus indicates the first listed vibration is more pronounced than the second. [f] neat powder between KBr plates; [g] KBr pellet. [h] Assignments related to the CS_3^+ ring are given in bold.

Table 2. Mass Spectral Data for the Recovered $PhCS_3Cl$[a]

m/*z* (obsd)[b]	intensity (%)[c]	*m*/*z* (calcd)[d]	assignment
64	27.7	64	S_2^+
66	1.8	66	$H_2S_2^+$ [e]
77	15.6	77	Ph^+
105	6.4	105	$PhCO^+$ [e]
121	100.0 (100)	121 (100)	$PhCS^+$
122	9.2 (9.2)	122 (8.4)	$PhCS^+$
123	6.6 (6.6)	123 (4.8)	$PhCS^+$
128	11.3	128	S_4^+
140	1.1	140	$PhCOCl^+$ [e]
156	19.8 (100)	156 (100)	$PhCSCl^+$
157	1.85 (9.3)	157 (8.4)	$PhCSCl^+$
158	4.1 (21)	158 (36.5)	$PhCSCl^+$
160	6.5	160	S_5^+
185	0.27	185	$PhCS_3^+$
188	0.63	188	$PhCO_2SCl^+$ [e]?
220	4.26 (100)	220 (100)	$PhCS_3Cl^+$
221	0.77 (18)	221 (10)	$PhCS_3Cl^+$
222	0.94 (22)	222 (46)	$PhCS_3Cl^+$
224	0.54	224	S_7^+
242	5.2	242	$Ph_2C_2S_2^+$
256	10.4	256	S_8^+

[a] Direct inlet, low-resolution, 25 °C, 27 eV. Peaks with intensities > 4% are listed. [b] Observed *m*/*z*. [c] Observed intensities with the scaled intensities in parentheses. [d] Calculated *m*/*z* for the assigned species, with the calculated isotopic distributions of the isotopomers (ref 61) included in parentheses. [e] Due to impurities.

Table 3. Observed (Calculated[a]) ^1H and ^{13}C NMR Chemical Shifts of **1** in Liquid SO_2 (Atom Labeling Given in Figure 2c)

	^{13}C				
	C1	C3 and C7	C4 and C6	C5	C2
δ_c	133.8 (135.2)	123.6 (125.6)	130.7 (135.6)	139.5 (153.3)	204.9 (213.7)
intensity[b]	8	89	100	53	5
	^1H				
		H3 and H7	H4 andH6	H5	
δ_H		7.87 d (7.88)	7.71, t (7.91)	7.98, tt (8.44)	
integration[c]		2	2	1	
J_{HH} (Hz)[d]	J(H5,H6) = J(H4,H5) = 7.6 J(H6,H7) = J(H3,H4) = 8.5 J(H5,H7) = J(H3,H5) = J(H4,H6) = J(H3,H7) = 1.2 J(H3,H6) = J(H4,H7) = 0.5				

[a] Isotropic NMR shielding tensors were calculated at the MPW1PW91/6-311G(2DF)//MPW1PW91/3-21g* level and referenced against calculated TMS values; d = doublet, t = triplet. [b] Relative peak heights given as relative intensities. [c] Observed integrated intensities. [d] Obtained by spin simulation (ABCDE spin system).

vibrational frequencies and assignments given in S-Table 5. The comparison of FT-Raman spectra of **14**Cl and **14**SbF_6 is given in S-Figure 9.

Synthesis of 14SbF$_6$. The dark brown **14**SbF_6 (0.663 g, 1.41 mmol, 94% yield) was prepared as described for **1**SbF_6 by the reaction of $AgSbF_6$ (0.609 g, 1.77 mmol) with **14**Cl (0.406 g, 1.50 mmol) in SO_2 (10.89 g) according to eq 10. The insoluble product was identified as AgCl by X-ray powder diffraction. Compound **14**SbF_6 gave a blue solution in SO_2, which gradually turned brown after 4 days at room temperature but remained blue after 16 days at 5 °C. An electron spin resonance (ESR) spectrum of the blue solution was recorded at room temperature and no signal was observed. The solubility of **14**SbF_6 is about 0.060 g/10 g SO_2 at room temperature. FT-Raman (4000−50 cm^{-1}) and FT-IR spectra (4000−400 cm^{-1}) of the purified **14**SbF_6 are shown in S-Figure 8, and assignments are given in S-Table 5. Attempts to grow crystals of **14**SbF_6 in liquid SO_2 were unsuccessful.

In situ ^1H, ^{19}F, and ^{13}C NMR spectra (about 10 mg of **14**SbF_6 in 1.5 g of SO_2 in a 5 mm NMR tube) of the above product were recorded as a function of time (10 min to 14 days) and are given in S-Figure 13. **14**SbF_6 gradually converted to unidentified species in liquid SO_2 after 14 days. The ^1H and ^{13}C NMR spectra of **14**SbF_6 were obtained within 10 min (^1H) and 1 day (^{13}C overnight) of preparation. The chemical shifts, integrations, coupling constants, and assignments are given in Table 4. The ^{19}F NMR spectrum of the solution was recorded at −70 °C after 1 day and is given in S-Figure 13c. ^{19}F NMR (400 MHz, SO_2): −71.09 (s, 3.0% F, ?), −108.1, −120.3 (two superimposed broad peaks, 94.0% F, SbF_6^-), −127.2 (s, 3.0% F, ?).

^1H NMR spectrum of the above isolated product revealed the presence of a small amount of impurities (S-Figure 13). A further purification of the brown **14**SbF_6 was conducted by recrystallization from liquid SO_2 followed by the removal of the most soluble components as described for the purification of **1**SbF_6. The ^1H NMR spectrum of the purified **14**SbF_6 (S-Figure 12) solution in SO_2 showed **14**SbF_6 and a broad peak which was probably due to the hydrolysis product since it was absent in the ^1H spectra of a sample which was prepared under vigorous dry conditions (S-Figure 13).

Results and Discussion

Synthesis of PhCS$_3$Cl. $PhCS_3Cl$ was prepared by the reported method according to eq 1 (Ar = Ph)[19] in about 40% yield. However, diethyl ether or a diethyl ether/CH_2Cl_2 mixture was used as a solvent instead of CCl_4. The purity of $PhCS_3Cl$ was monitored by FT-Raman spectroscopy. It is important to carry out the filtration immediately after addition of the acid and to use distilled SCl_2 in 10−20% excess; otherwise the product was a red viscous oil. The yields were higher when diethyl ether, rather than CH_2Cl_2/diethyl ether or CCl_4/diethyl ether, was used as the solvent. The initially formed precipitate $PhCS_3Cl$ (FT-Raman) disappeared very rapidly in the CH_2Cl_2/ether or CCl_4/ether solvents, giving $Ph_2C_2S_3Cl_2$[20] as the major recovered product (from the filtrate). These observations suggested the formation of $Ph_2C_2S_3Cl_2$[20] according to eq 2 was less rapid in diethyl ether, probably because of the higher solubility of $PhCS_3Cl$ in CH_2Cl_2 and CCl_4 than in diethyl ether, in which it appears to be insoluble.

$$2\ PhCS_3Cl \rightarrow Ph_2C_2S_3Cl_2 + 3/8\ S_8 \qquad (2)$$

Synthesis of 1MF$_6$ by the Reaction of PhCS$_3$Cl and AgMF$_6$ (M = As, Sb). **1**MF_6 (M = As, Sb) was synthesized according to eq 3. To minimize the decomposition of $PhCS_3Cl$ in SO_2, $AgSbF_6$ was first dissolved in liquid SO_2 and then added to $PhCS_3Cl$ and the resulting mixture was stirred. The reaction of $AgSbF_6$ and $PhCS_3Cl$ reached completion within 0.5 h. The product was recovered in no more than 2 h since **1**SbF_6 gradually converts to **2**$(SbF_6)_2$.[20]

$$PhCS_3Cl + AgMF_6 \xrightarrow[M = As, Sb]{SO_2} \mathbf{1}MF_6 + AgCl \qquad (3)$$

1AsF_6 (FT-Raman) was synthesized similarly. It was also detected by ^1H NMR as the major product (40−54% H) of the oxidation of $Zn(PhCS_2)_2$ by AsF_5 in an attempt to

Table 4. Observed[a] (in **14**SbF_6) and Calculated[b] (in Parentheses) ^1H and ^{13}C NMR Chemical Shifts of **14** (Atom Labeling Given in Figure 2b)

					^1H						
	C1−H	C3−H	C4−H	C5−H	C6−H	C7−H	C8−H	C9−H	C10−H	C11−H	C2−H
δ_H		8.36 d	8.02 t	8.87 d	8.84 d	8.03 t	8.25 t	8.76 dd			
calcd		(8.19)	(7.88)	(8.82)	(8.52)	(8.25)	(8.41)	(8.22)			
integration[c]		1H	1H	1H	1H	1H	1H	1H			
J(H,H) (Hz)[d]		8.0	7.6	8.0	8.0	7.6	8.0	8.0, 0.8			
naphthalene	7.66	7.30	7.30	7.66	7.66	7.30	7.30	7.66			
					^{13}C						
	C1	C3	C4	C5	C6	C7	C8	C9	C10	C11	C2
δ_c	135.5	125.2	129.2	151.3	137.4	134.1	143.8	132.3	131.0	131.5	207.4
calcd	(134.7)	(126.8)	(128.9)	(154.9)	(140.2)	(136.0)	(142.7)	(133.3)	(133.3)	(137.6)	(207.4)
intensity[e]	34	94	92	82	99	77	97	100	13	13	13
naphthalene	127.7	125.6	125.6	127.7	127.7	125.6	125.6	127.7	133.3	133.3	

[a] Spectra were obtained at room temperature (solvent: liquid SO_2), using TMS in liquid SO_2 as an external standard. [b] Isotropic NMR shielding tensors were calculated at the MPW1PW91/6-311G(2DF)//MPW1PW91/3-21g* level and referenced against calculated TMS values; d = doublet, t = triplet. [c] Observed integrations. [d] Experimental values. [e] Relative peak heights given as relative intensities.

synthesize **2**$(AsF_6)_2$ according to proposed eq 4. A discussion of this synthesis is included in the Supporting Information.

$$8\ Zn(PhCS_2)_2 + 48\ AsF_5 \xrightarrow{SO_2} 8\ \mathbf{2}(AsF_6)_2 + S_8 + 8\ Zn(AsF_6)_2 + 16\ AsF_3 \quad (4)$$

Characterization of $1MF_6$ (M = As and Sb). The identify of **1**MF_6 was established from elemental analysis for all elements, ^1H, ^{13}C, ^{19}F NMR, and vibrational spectroscopy and from a preliminary X-ray crystal structure of **1**SbF_6 which confirmed the atomic connectivity of **1**. In addition, theoretical calculations were in satisfactory agreement with the experimental spectroscopic and structural data.

(a) Structure and a Preliminary Analysis of the Bonding in 1. A preliminary X-ray crystal structure of **1**SbF_6 was obtained, confirming the atomic connectivity of **1**. The observed geometry of **1** is shown in Figure 2c. The CS_3^+ ring is planar (dihedral angle (ϕ) of C2−S3−S4−S5 = 0.40(1)°) and coplanar with the average mean plane of the phenyl ring (angle between the two planes = 3.5°), consistent with the optimized geometry of **1**, in which the rings are planar and the angle between the planes is 0.01° (MPW1PW91/3-21G*) or 8.73° (MPW1PW91/6-31G*). The bond angles and bond distances in the four-membered ring are consistent with the calculated values (Figure 2d) and those observed in **3**[5] (Figure 2e) except for the $C-CS_3$ single bond (1.524(3) Å), which is much longer than that in **3** (1.450(8) Å) and the calculated distance (1.421 Å). The large R value (R1 = 10.3%) and problems arising from twinning preclude a detailed discussion of the geometry of **1**SbF_6. Attempts to obtain single crystals of **1**AsF_6 and **1**SbF_6 were unsuccessful.

The Pauling bond orders[36] (based on the observed bond distances) and/or calculated Wiberg bond orders (MPW1PW91/6-31G*//MPW1PW91/3-21G*) for the bonds in the $C-CS_3^+$ portion of HCS_3^+, $PhCS_3^+$, and **3** are given in Table 5. Pauling bond orders are in agreement with the calculated Wiberg bond orders except that for the $C-CS_3^+$ bond of the observed **1** given by the preliminary X-ray structure which is undoubtedly incorrect. The bond orders indicate that resonance structures of **c** and **d** contribute the most to the overall bonding in RCS_3^+ (resonance structures **a**−**e**, given in Chart 1). Consistently, the calculated charges are higher on S3 and S5 than on S4 (Table 5). The sums of valence units[37] based on the cation−anion contact distances (from the X-ray crystal structure of **3**$(AsF_6)_3$)) are very similar for the three atoms (S3 0.42, S4 0.40, and S5 0.36) (Table 5). The calculated negative charge on C2 and positive charge on S4 imply that the rather improbable valence bond structures **a** and **b** in Chart 1 might make some contribution to the overall bonding in **1**. The sum of the bond orders of the bonds in $-CS_3^+$ is approximately 5 ($4\sigma + 1\pi$) consistent with a 6π electronic structure. The calculated and observed ∠SSS are less than 83.1°, to the best of our knowledge, the smallest SSS bond angle observed in an isolated compound [cf. ∠SSS in S_8 is 107.30(2)°],[38] and the ∠SCS (ca. 107°) is less than the ideal 120°. Thus, the CS_3^+ ring is strained. The observed trans ring distances C2−S4 and S3−S5 (2.57/2.70 Å in **1** and 2.54/2.72 Å in **3**) are much less than the sum of the van der Waals radii of the corresponding atoms (3.45 and 3.60 Å) and correspond to the calculated Wiberg bond orders of 0.1−0.2 and 0.2−0.3, respectively.

The calculations showed that when H in HCS_3^+ is replaced by phenyl or 1-naphthyl, the C−S bonds lengthen and the C1−C2 distance (Figure 2) has a bond order greater than 1 (Table 5), reflecting the contribution of resonance structures of type **1f**, **1g**, and **1h** to the overall bonding in **1**, which are absent for HCS_3^+. The calculated NBO charges on the sulfur atoms in **1** and **14** are very similar to each other but smaller than those in HCS_3^+, consistent with delocalization of the positive charge into the phenyl and 1-naphthyl rings.

The HCS_3^+ (C_{2v}) π molecular orbitals (MOs) are very similar to those of S_4^{2+} (D_{4h})[39] (Figure 3). The major

(36) The Pauling bond order is given by a variation of Pauling's bond distance−bond order relationship (ref 66), $D(n') = D_1 - 0.71 \log n'$ where $D(n')$ is the observed bond distance and D_1 is the single bond distance (D_1(S−S) 2.08 Å, D_1(C−S) 1.81 Å, and $D_1(C_{sp2}-C_{sp2})$ 1.48 Å).

(37) Brown, I. D. In *Structure and Bonding in Crystals*; O'Keefe, M., Navrotsky, A., Eds.; Academic Press: London, 1981.
(38) Cameron, T. S.; Decken, A.; Dionne, I.; Fang, M.; Crossing, I.; Passmore, J. *Chem.—Eur. J.* **2002**, *8*, 3386−3401.
(39) Krossing, I.; Passmore, J. *Inorg. Chem.* **1999**, *38*, 5203−5211.

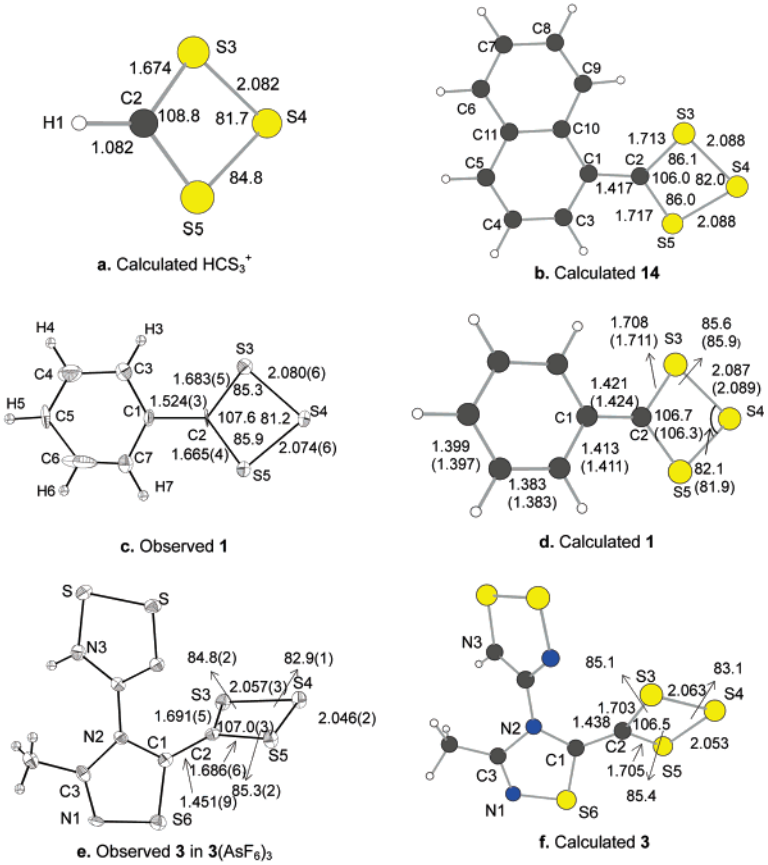

Figure 2. Selected observed or calculated (MPW1PW91/3-21G* and/or MPW1PW91/6-31G* (in parentheses)) bond distances (Å) and angles (deg) of HCS_3^+, **14**, **1**, and **3**. Thermal ellipsoid plots of **1** and **3** are drawn at the 25% probability level. (a) HCS_3^+: C2−S4, 2.550; S3−S5, 2.723; S4−C2−S3−H1, 180.0; C2−S3−S4−S5, 0.0. (b) Calculated **14**: C2−S4, 2.608; S3−S5, 2.739; C1−C2−S5, 125.0; C1−C2−S3, 128.9; C1−C2−S3−S5, 176.4 (177.0); C2−S3−S4−S5, 1.1 (1.2); naphthyl ring (planar)/CS_3^+ ring, 19.8 (20.3). (c) Observed **1** (from a preliminary X-ray crystal structure of **1**SbF_6): C2−S4, 2.565(5); S3−S5, 2.703(2); C1−C2−S5, 125.72(2),; C1−C2−S3, 126.63(2); C1−C2−S3−S5, −179.69(3); C2−S3−S4−S5, 0.40(1); C2−C1−C3−C4, 179.90(3); Ph ring/CS_3^+ ring, 3.5. (d) Calculated **1**: C2−S4, 2.594; S3−S5, 2.741; S3−C2−C1−S5, 180.0 (180.0); C1−S5−S4−S3, 0.00 (0.00); Ph ring/CS_3^+ ring, 0.01 (8.73). (e) Observed **3**: C2−S4, 2.542(7); S3−S5, 2.715(2); C1−C2−S5, 124.9(5); C1−C2−S3, 127.4(5); C1−C2−S3−S5, −170.8(8); C2−S3−S4−S5, 0.4(2); C1N2C3N1S6 ring (planar)/CS_3^+ ring, 108(1). (f) Calculated **3**: C2−S4, 2.560; S3−S5, 2.729; C1−C2−S5, 122.7 (123.2); C1−C2−S3, 130.1 (129.5); S3−C2−S5, 106.5 (106.6); C2−S3−S4, 85.1 (85.2); S3−S4−S5, 83.1 (82.8); C1−C2−S3−S5, 171.8 (170.4); C2−S3−S4−S5, 0.76 (0.21); C1N2C3N1S6 ring (planar)/CS_3^+ ring, 39.4 (130.6).

difference is that the two nonbonding orbitals (HOMO and HOMO-1) of HCS_3^+ are not degenerate due to the lower symmetry of HCS_3^+. The three π bonding orbitals of the phenyl ring (as in benzene)[40] interact with the three occupied π type orbitals of $-CS_3^+$ (as in HCS_3^+), forming six occupied π orbitals of **1** as shown in Figure 4. The LUMO of **1** is antibonding as in HCS_3^+. Three π MOs of **1** (HOMO-2, HOMO-7, and HOMO-11) have π bonding character in the $C-CS_3^+$ bond, and one π MO (HOMO) has anti π bonding character (the p_z orbital coefficients are given in S-Table 8). Thus, there is an overall net π bonding in the $C-CS_3^+$ bond. Similar analysis suggests that there is net π bonding in the S−S bonds and the C−S bonds (S-Table 8), the latter greater than the former, in agreement with the bond order analysis given above. Thus, the MO analysis implies some aromatic characteristics for the CS_3^+ ring in **1**, consistent with the presence of 6 π electrons in the $-CS_3^+$ ring, although the π bonding is predominantly in the SCS region. The S−S bond orders in **1** and **3** are only very slightly greater than 1, probably due to bond weakening attributable to the ring strain (see above).

(b) ^{1}H and ^{13}C NMR Studies. In situ ^{1}H NMR study of a **1**SbF_6 solution in liquid SO_2 (concentration: 0.12 mmol/g SO_2) showed 4 mol % of **1**SbF_6 converted to **2**$(SbF_6)_2$ (via intermediate **12** or **13**) and S_8 in 10 min and about 60 mol % after **14** days at room temperature according to eq 5. Detailed information is given in S-Figure 10. The ^{1}H spectrum of **1**SbF_6 in SO_2 (S-Figure 10) was obtained immediately after the sample preparation, and the ^{13}C {1H} NMR spectrum (S-Figure 11) was obtained over 12 h after sample preparation. The integral ratios and peak profiles of the ^{1}H spectrum and the intensities of the peaks in the ^{13}C spectrum of **1** (Table 3) were as expected. The peak due to the quaternary C1 (atom labeling given in Figure 2c) was distinguished from the others by its much lower intensity caused by the absence of a nuclear overhauser effect. The ortho and meta carbons are assigned based on the general observation that the chemical shifts of ortho carbons are more affected (greater deviation from the 128.5 ppm of benzene carbons) than those of meta carbons by substituent effects (e.g., the inductive effect, the resonance effect, and the

(40) Fleming, I. *Frontier Orbitals and Organic Chemical Reactions*; Wiley-Interscience: London, 1976.

Table 5. Pauling Bond Orders (PBO) (Based on the Observed Bond Distances in X-ray Crystal Structures) and/or Calculated Wiberg Bond Orders (WBO) (MPW1PW91/6-31G*//MPW1PW91/3-21G*), Calculated NBO Charges (MPW1PW91/6-31G*//MPW1PW91/3-21G*), and/or Sum of Valence Units[a] (Based on X···F Contact Distances (X = C and S) Derived in the X-ray Crystal Structure) for the C(or H)−CS_3^+ Ring Fragment

Bond Orders

		calculated WBO			experimental PBO	
bond	HCS_3^+	**14**	**3**	**1**	**1**	**3**
H1−C2	0.85					
C1−C2		1.23	1.13	1.20	0.87(1)	1.10(3)
C2−S3	1.42	1.26	1.27	1.30	1.51(2)	1.47(2)
S5−C2		1.25	1.29		1.60(2)	1.50(3)
S3−S4	1.06	1.01	1.09	1.04	1.00(2)	1.08(1)
S4−S5		1.02	1.11		1.02(2)	1.12(1)
C2−S4	0.16	0.10	0.17	0.12	0.09	0.09
S3−S5	0.25	0.14	0.26	0.17	0.13	0.13

Charges

		NBO			sum of valence units of cation−anion contacts in **3**
	HCS_3^+	**14**	**3**	**1**	
H1	0.34				
C1		−0.13	−0.06	−0.17	0.03
C2	−0.66	−0.39	−0.57	−0.36	0.02
S3	0.57	0.46	0.61	0.48	0.42
S5	0.57	0.45	0.64	0.48	0.36
S4	0.19	0.13	0.35	0.16	0.40

[a] Contacts less than the sum of the van der Waals radii (Å) (ref 63) were included (S···F ≤ 3.40, C···F ≤ 3.30). The bond valence *S* in valence units (vu) is given by $S = (R/R_0)^{-N}$, where *R* is the observed contact distance (Å), $R_0 = 1.55$ Å, and $N = 3.8$ for S^{IV}···F (ref 37). The bond valences of C are given by $S = \exp((R_0 - R)/B)$, $B = 0.37$, *R* is the observed bond distance (Å), R_0 is 1.32 for C···F (ref 64).

electric field effect).[41] The dithio carbon (C2) assignment is unequivocal as the chemical shifts of the dithio carbons in ArC(S)SH and ArC(S)SCH_3 are above 200 ppm.[42] The ^{13}C chemical shift of the C in the CS_3^+ ring in **1** (204.9 ppm) is also similar to those in compounds $[R-C(SMe)_2]^+$ (**16** and **17**) (208−219 ppm).[43] The calculated ^1H and ^{13}C NMR chemical shifts are in reasonable agreement with the above assignments (Table 3).

The ^{19}F NMR spectrum of **1**SbF_6 in liquid SO_2 at room temperature showed a 10 line multiplet at −115 ppm,[44] arising from couplings of ^{19}F with ^{121}Sb ($I = 5/2$, a sextet) and ^{123}Sb ($I = 7/2$, an octet), rather than the usual broad line,[45,46] indicating slow cation−anion exchange.

$$2\ \mathbf{1}SbF_6 \rightarrow 3/8\ S_8 + \mathbf{2}(SbF_6)_2 \qquad (5)$$

(c) Vibrational Spectra of 1MF_6 (M = As, Sb). The FT-Raman spectra of **1**MF_6 salts in the region of 1650−50 cm^{-1} are shown in Figure 1, and the IR spectrum of **1**SbF_6 is given in S-Figure 3 (instrumental cutoff: Raman ≈ 50 cm^{-1}; IR ≈ 400 cm^{-1}); frequencies, intensities, and assignments are listed in Table 1. The assignments for As/SbF_6^- were made by comparison with AsF_6^- ($CsAsF_6$, N_5AsF_6, $M_3X_3AsF_6$ (M = S, Se; X = Cl, Br)) and SbF_6^- ($LiSbF_6$, N_5SbF_6, $M_3X_3SbF_6$ (M = S, Se; X = Cl, Br) salts.[28,47,48] The MF_6^- bands were relatively weak compared to those attributed to **1**, which were identical in both salts (Figure 1).

The assignments for **1** were made based on the spectra calculated using the 6-31G* basis set without geometry restriction[49] and are given in Table 1. Thirty-nine vibrational modes are expected for **1** (illustrated in S-Figure 14), among which 30 vibrational modes are due to the phenyl ring, which

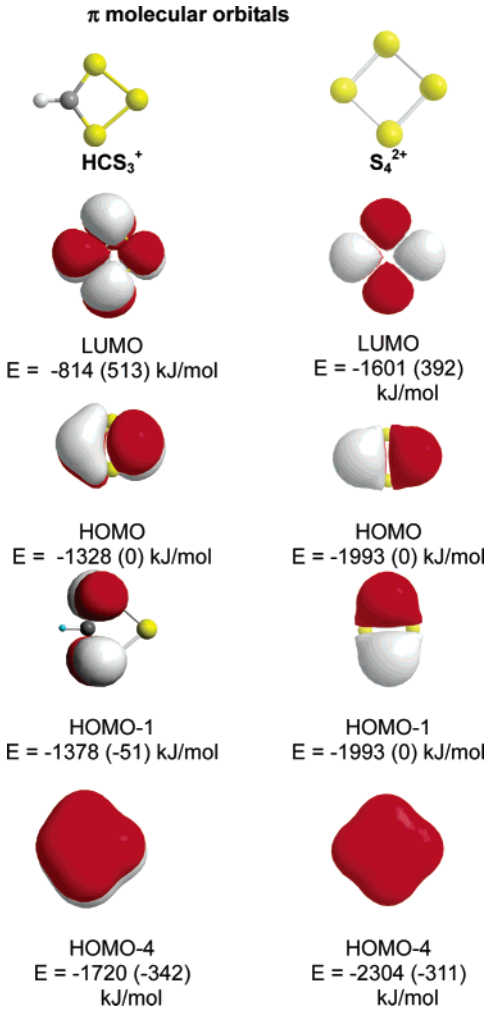

Figure 3. A comparison of π type molecular orbitals (isosurface drawn at 0.01 au) of HCS_3^+ (MPW1PW91/6-311+G(d)) and S_4^{2+} (B3PW91/6-311+G(d)). Data in the parentheses are energies relative to that of HOMO. The HOMO-2 and HOMO-3 molecular orbitals are of the σ type and are included with the Supporting Information.

(41) Breitmaier, E.; Voelter, W. *Carbon-13 NMR Spectroscopy*: *High-Resolution methods and appplications in organic chemistry and Biochemistry*, 3rd ed.; VCH: New York, 1987.
(42) Jabre, I.; Saquet, M.; Thuillier, A. *J. Chem. Res.* **1990**, *4*, 756−784.
(43) Coustard, J. M. *Tetrahedron* **1995**, *51*, 10929−10940.
(44) The ^{19}F of **1**SbF_6 in liquid SO_2 was taken after 7 days (S-Figure 18, top); at this time, the ratio of **1**SbF_6, **2**$(SbF_6)_2$, and **12**$(SbF_6)_2$ or **13**$(SbF_6)_2$ was 67:10:6.5 according to its corresponding ^1H spectrum (S-Figure 18, bottom). Therefore the peaks observed in ^{19}F are mainly due to **1**SbF_6. The SbF_6^- in **2**$(SbF_6)_2$ and **12**$(SbF_6)_2$ or **13**$(SbF_6)_2$ probably gave the same pattern at the same chemical shift as that of the SbF_6^- in **1**SbF_6^- since the overall shapes of the peaks are very similar to those due to the SbF_6^- (−123 ppm) of $AgSbF_6$ in acetonitrile (14 peaks resolved) reported by Matthews et al. (ref 45).
(45) Kidd, R. G.; Matthews, R. W. *Inorg. Chem.* **1972**, *11*, 1156−1157.
(46) Christe, K. O.; Schack, C. J.; Wilson, I. L. *Inorg. Chem.* **1975**, *14*, 2224−2230.
(47) Begun, G. M.; Rutenberg, A. C. *Inorg. Chem.* **1967**, *6*, 2212−2216.
(48) Vij, A.; Wilson, W. W.; Vij, V.; Tham, F. A.; Sheehy, J. A.; Christe, K. O. *J. Am. Chem. Soc.* **2003**, *123*, 6308−6313.

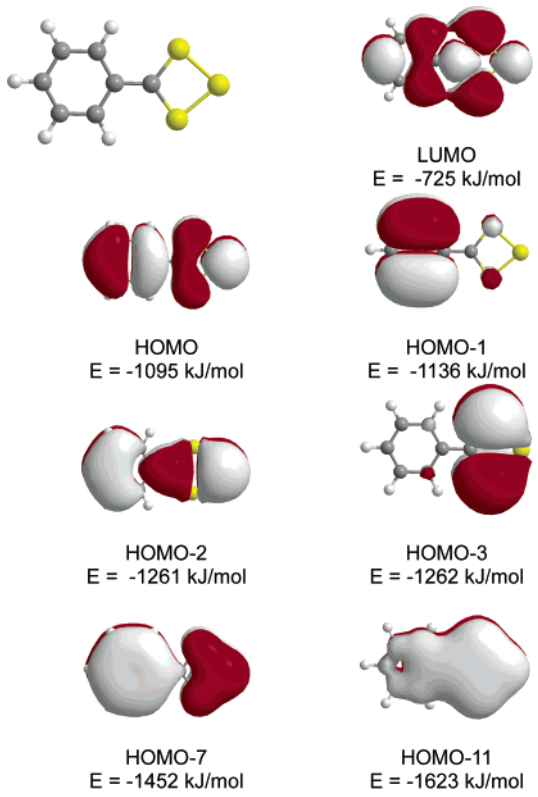

Figure 4. The π type molecular orbitals of **1** calculated at the MPW1PW91/6-31G* level (isosurface drawn at 0.01 au).

are very similar to the corresponding vibrational bands observed for monosubstituent phenyl rings in Ph−X (X = F, Cl, Br, I, CH_3),[50] $KPhCS_2$,[51,52] and $In(PhCS_2)_3$[51,52] (Table 1) except for the substituent-sensitive modes (ω_6, ω_{10}, ω_{11}, ω_{24}, ω_{29}, ω_{30}).[50,53] The remaining 9 vibrational modes (calculated) arise from the CS_3^+ ring.

The calculated vibrational frequencies and intensities for $PhCS_2^-$ using the same method as that for **1** agree reasonably well with the previously reported[51,52] values and assignments for $KPhCS_2$ and $In(PhCS_2)_3$ (Table 1) with a few revisions based on the calculated results. There is also good agreement with the calculated and experimental results for the phenyl group vibrations of **1**.

Taking into account that the peak intensities of gas-phase spectra can be different from those in the solid state and that some peaks split in the solid state, there is a good correlation between the observed and calculated frequencies and intensities. One notable difference is the CH stretches of the phenyl ring were invisible in the FT-Raman spectra while the calculation predicts strong Raman activities. However, the intensities of aromatic υ(CH) stretches in the liquid or solid Raman spectra of some substituted benzene compounds are weak or nearly invisible (e.g., FT-Raman spectra of 2,4,6-trinitrophenol and 2,4-dinitrophenol).[54,55] We note that the C−H vibrations for solid-state $KPhCS_2$ and $In(PhCS_2)_3$ were also not reported in either IR and Raman spectra.[52]

The weak Raman peak at 483 cm^{-1} is assigned to the CS_3 ring deformation. The medium strong peak at 534 cm^{-1} (calcd: 515 cm^{-1}) in the FT-Raman spectrum of **1**SbF_6 is assigned to the superimposition of the symmetric CS_3 ring breathing (involving the symmetric υ(SSS) stretch) and asymmetric υ(SSS) stretching modes since the calculated vibrational frequencies for these two modes have identical values. The 534 cm^{-1} (cf. 473 cm^{-1} in S_8)[38] vibration does not only consist of the S−S stretching mode, but nevertheless the corresponding S−S distance of 2.00 Å as estimated from eq 6[28] is in rough agreement with that observed in **3** [av 2.052(2) Å] and shorter than the S−S single bond distance (2.08 Å) in C−SS−C containing compounds with the C−S−S−C dihedral angle of 0°.[56]

$$\nu(\mathrm{S-S})/\mathrm{cm}^{-1} = 3060 - 1263\, d(\mathrm{S-S})/\text{Å} \qquad (6)$$

Vibrational frequencies due to the CS_2 fragments in **1**SbF_6 (υ_{sym} 962 cm^{-1}, υ_{asym} 999 cm^{-1}) are similar to those of $M(PhCS_2)_2$ (M = Ni(II) and Pd(II)) salts (υ_{sym} 941−947 cm^{-1}, υ_{asym} 973−992 cm^{-1})[51] and are in the range between the vibrational frequencies for a υ(C−S) stretch (~670 cm^{-1}) and a υ(C═S) stretch (~1250 cm^{-1}),[57] indicating resonance structures of **c** and **d** contribute significantly to the overall bonding in **1**.

The strong bands at 1301 and 1317 cm^{-1} observed in both the IR and Raman spectra is assigned to a substituent-sensitive vibration mode, ω_6 (mainly the υ(Ph−C) stretching vibration)[50] of the phenyl group. The υ(Ph−C) stretches of the metal complexes of $ArCS_2^-$ (e.g., $Ni(PhCS_2)_2$, $Pd(PhCS_2)_2$, $Cr(PhCS_2)_2$, and $Fe(PhCS_2)_2$) are also strong in both the IR and Raman and lie between 1246 and 1273 cm^{-1}.[51,58] The bands at 1301 and 1317 cm^{-1} corresponds to a C−C bond distance of 1.43−1.44 Å as estimated from eq 7,[59] shorter than a single C_{sp2}−C_{sp2} (1.48 Å),[60] which is in agreement with the calculated bond distance of the Ph−C

(49) The calculated vibrational spectra of **1** at different basis sets (3-21G* or 6-31G*) with C_{2v} geometry or without geometry restriction are compared in S-Table 6. The energy difference between the optimized **1** (MPW1PW91/6-31G*) with C_{2v} and without symmetry restriction is 0.12 kJ/mol. The spectrum calculated using the 3-21G* basis set is similar to those calculated using the 6-31G* basis set. The calculated frequencies and intensities using the 6-31G* basis set based on optimized geometries with C_{2v} symmetry or without symmetry restriction are nearly identical except that the first frequency of the C_{2v} geometry is a negative value indicating the C_{2v} geometry is not a stationary point.

(50) Schmid, E. W.; Brandmüller, J.; Nonnenmacher, G. *Z. Elektrochem.* **1960**, *64*, 726−733.
(51) Maltese, M. *J. Chem. Soc., Dalton Trans.* **1972**, 2664−2667.
(52) Mattes, V. R.; Stork, W.; Pernoll, I. *Z. Anorg. Allg. Chem.* **1974**, *404*, 97−102.
(53) Whiffen, D. H. *J. Chem. Soc.* **1956**, 1350−1356.
(54) Carreira, L. A.; Towns, T. G. *J. Mol. Struct.* **1977**, *41*, 1−9.
(55) Passingham, C.; Hendra, P. J.; Hodges, C.; Willis, H. A. *Spectrochim. Acta* **1991**, *47A*, 1235−1245.
(56) McCormack, K. L.; Mallinson, P. R.; Webster, B. C.; Yufit, D. S. *J. Chem. Soc., Faraday Trans.* **1996**, *92*, 1709−1716.
(57) Bak, B.; Hansen-Nygaard, L.; Petersen, C. *Acta Chem. Scand.* **1958**, *12*, 1451.
(58) Burke, J. M.; Fackler, J. P. *Inorg. Chem.* **1972**, *11*, 3000−3009.
(59) The stretching frequencies for a single C−C (1.53 Å in ethane) and a double C═C bond (1.34 Å) are 993 and 1623 cm^{-1}, respectively. Assuming the C−C stretching frequencies and bond distances have a linear relationship, eq 7 was derived. The υ(C≡C) of HC≡CCH_3 is 2130 cm^{-1}. The corresponding bond distance of C≡C deduced from eq 7 is 1.19 Å, close to the standard 1.20 Å for the C≡C distance.
(60) March, J. *Advanced Organic Chemistry*: *Reactions, Mechanisms, and Structure*, 4th ed.; John Wiley & Sons Ltd.: New York, 1992.

bond (1.421 Å). This indicates that the resonance structures **1f**, **1g**, and **1h** also contribute to the overall bonding in **1**.

$$\nu(\mathrm{C-C})/\mathrm{cm}^{-1} = 6066 - 3316\, d(\mathrm{C-C})/\text{Å} \qquad (7)$$

Characterization of $PhCS_3Cl$. $PhCS_3Cl$ was obtained as a yellow precipitate from the reaction of $PhCS_2H$ and SCl_2 in diethyl ether. The purity of $PhCS_3Cl$ was confirmed by its melting point (mp 90−93 °C; reported[19] 90−92 °C with excellent elemental analyses for all elements). The IR frequencies were also consistent with the literature values; however only the bands in the region of 1180−2330 cm^{-1} were reported.[19] The product prepared according to Campaine et al.'s procedure[19] in CCl_4/diethyl ether had the same FT-Raman spectrum as that of the $PhCS_3Cl$ prepared in CH_2Cl_2/diethyl ether or only diethyl ether as the solvent. This confirmed that a product identical to that of Campaine et al. had been prepared. Attempts to obtain NMR spectra of $PhCS_3Cl$ (in $CDCl_3$ and SO_2) were unsuccessful.

(a) Mass Spectra. Mass spectral data of $PhCS_3Cl$ obtained at 70 eV were consistent with those reported by Campaine et al.[19] The fragments attributable to $PhCS_3^+$ (185, 0.27%) and the molecular ion $PhCS_3Cl^+$ (219.9, 4.26%) were observed for the first time with a lower ionization power (27 eV). The isotopic distributions for $PhCS^+$, $PhCSCl^+$, and $PhCS_3Cl^+$ fit well with the expected values (Table 2).[61] The above results are in agreement with the formulation of $PhCS_3Cl$ and suggest that $PhCS_3Cl$ is monomeric and covalent in the gas phase, probably with a structure of **19** or **20**. **20** is preferred as S_xCl^+ ions were not detected (x = 1−2).

The observation of fragments possibly due to $PhCO^+$ (105.1, 5.4%), $PhCOCl^+$ (140.0, 1.1%), and $PhCO_2SCl^+$ (188.0, 0.63%) suggested the presence of traces of PhCOSOCl, **15**Cl. However, the attempted synthesis by the reaction of $PhCO_2H$ and SCl_2 was unsuccessful. Observed fragments assigned to S_4^+, S_5^+, S_7^+, S_8^+, and $Ph_2C_2S_2^+$ (242.0, 5.2%) were attributed to S_8 and $Ph_2C_2S_3Cl_2$, likely produced by the conversion of $PhCS_3Cl$ to $Ph_2C_2S_3Cl_2$ and S_8 on heating according to eq 2, by analogy to the conversion of **1**SbF_6 to **2**$(SbF_6)_2$ in liquid SO_2.[20]

(b) Reaction Evidence for the Structure of $PhCS_3Cl$. The $PhCS_3^+Cl^-$ structure was strongly implied by the reversible interconversions between $PhCS_3Cl$ and **1**SbF_6. The reaction of **1**SbF_6 and NBu_4Cl in liquid SO_2 immediately produced a yellow precipitate (eq 8), which was identified as $PhCS_3Cl$ (FT-Raman spectrum shown in S-Figure 6). The obtained $PhCS_3Cl$ reacted readily with $AgSbF_6$ in liquid SO_2 to give AgCl (X-ray power diffraction) and **1**SbF_6 (eq 3) (FT-Raman and ^1H spectra (S-Figure 5)).

$$NBu_4Cl + \mathbf{1}SbF_6 \rightarrow NBu_4SbF_6 + PhCS_3Cl \qquad (8)$$

(c) Structural Implications of the Vibrational Spectra of $PhCS_3Cl$. The FT-Raman spectrum in the region 1650−50 cm^{-1} is compared with those of **1**MF_6 in Figure 1. The FT-Raman spectrum in the range 4000−50 cm^{-1} and FT-IR spectra (4000−400 cm^{-1}) of $PhCS_3Cl$ are shown in S-Figure 2. The frequencies and assignments of the vibrational spectra of $PhCS_3Cl$ are given in Table 1.

The vibration spectra of $PhCS_3Cl$ and the $PhCS_3^+$, **1**, in $PhCS_3MF_6$ (M = As, Sb), **1**MF_6, are similar implying that the former compound is largely ionic. However, the intensities of the CS_3^+ ring breathing and SSS stretching vibration in $PhCS_3Cl$ are very different from those of **1**MF_6, probably due to the much stronger anion−cation interactions in the former. A discussion is included in the Supporting Information.

Syntheses of 14Cl and 14SbF_6. (a) Synthesis of 14Cl. Orange **14**Cl was prepared according to eq 9 as described for the synthesis of $PhCS_3Cl$ (above) and as previously reported.[19] **14**Cl, like $PhCS_3Cl$, is not extremely air-sensitive; however, the peaks in the FT-Raman spectrum decreased in intensity on exposure to air for 1 day. Diethyl ether was a better solvent for the synthesis than a mixed solvent of CH_2Cl_2 and diethyl ether. However, the difference was not as great as in the case of $PhCS_3Cl$. A yield of 74% was obtained when using diethyl ether as solvent, compared to 59% when using CCl_4/diethyl ether.[19]

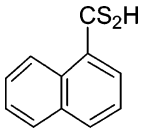

$$+ SCl_2 \longrightarrow C_{10}H_7CS_3Cl + HCl \qquad (9)$$

(b) Synthesis of 14SbF_6. The dark brown powder **14**SbF_6 was prepared from the reaction of **14**Cl with $AgSbF_6$ as described for **1**SbF_6 according to eq 10. The yield (94% assuming **14**SbF_6) was much higher than that of **1**SbF_6 (40−48%). The red insoluble product (0.159 g, 1.11 mmol assuming AgCl; expected: 0.20 g) was mainly AgCl (X-ray powder diffraction).

$$C_{10}H_7CS_3Cl + AgSbF_6 \rightarrow \mathbf{14}SbF_6 + AgCl \qquad (10)$$

Characterization of 14SbF_6. (a) ^1H and ^{13}C NMR Spectroscopy. The assignments of the ^1H and ^{13}C chemical shifts of **14**SbF_6 are given in Table 4. The observed and calculated chemical shifts (MPW1PW91/6-311G(2df)//MPW1PW91/3-21G*) are in reasonable agreement. Detailed arguments for the assignments are included in the Supporting Information.

(b) Vibrational Spectra of 14SbF_6. FT-IR (4000−400 cm^{-1}) and FT-Raman (4000−50 cm^{-1}) spectra of **14**SbF_6 are shown in S-Figure 8. The assignments were made based on the calculated spectra at the MPW1PW91/6-31G* level and are given in S-Table 5. The calculated frequencies and intensities using the 3-21G* basis set are similar to those calculated with the 6-31G* basis set (S-Table 7). The depictions of the calculated vibrational modes of **14** are shown in S-Figure 15. The observed and calculated frequencies are in reasonable agreement, supporting the identity of **14**SbF_6.

The CS_3 ring breathing vibration of **14**SbF_6 appeared at 513 cm^{-1} (m), similar to that of **1**MF_6 (534 cm^{-1} (m)). The

(61) The expected isotopic distributions are calculated by the software provided by the following web site: http://www.shef.ac.uk/chemistry/chemputer/isotopes.html.

$\upsilon(CS_2)$ stretches were found at 906 (sym) and 966 (asym) cm^{-1} in the FT-Raman spectrum, at slightly lower frequencies than those in **1**SbF_6 (962 (sym), 999 cm^{-1} (asym)).

Characterization of 14Cl. (a) Mass Spectrometry. The mass spectrum (28 eV) of **14**Cl and assignments are listed in S-Table 4. Fragments due to $[\mathbf{14}Cl]^+$ 270 (0.09%), $[\mathbf{14}]^+$ 234 (0.13%), $[C_{10}H_7CSCl]^+$ 204 (9.8%), and $[C_{10}H_7CS]^+$ 171 (82%) were observed, consistent with the mass spectrum of $PhCS_3Cl$ (see Table 2). In addition, S_2Cl^+ [99 (77%)] and SCl^+ [67 (47%)] peaks were also detected, implying stronger $Cl^-\cdots S$ contacts compared to those of $PhCS_3Cl$ and/or decomposition prior to evaporation in the direct inlet probe.

(b) Vibrational Spectroscopy. The FT-IR (4000−400 cm^{-1}) and FT-Raman spectra (4000−50 cm^{-1}) of **14**Cl are shown in S-Figure 7, and the vibrational frequencies and assignments given in S-Table 5. The spectra are assigned by comparison with the calculated vibrational frequencies of **14**. The vibrational spectra of **14**Cl correlate well with those of **14**SbF_6, indicating similar structures (S-Table 5 and S-Figure 9).

Conclusions

The trithietanylium heterocyclic cation, formally 6π RCS_3^+, is of fundamental interest as a simple small ring species. It is a member of a class of four-membered rings that includes $(RC)_4^{2-}$ and S_4^{2+}, shown in Scheme 1. We serendipitously prepared[5] the first example of this ring system in the complex tricyclic **3** prepared in very low yield from the reaction of sulfur homopolyatomic cations and CH_3CN. In 1968 Campaine et al.[19] reported the preparation of $ArCS_3Cl$ (R = Ph and aryls) and provided some evidence for an ionic cyclic $ArCS_3^+Cl^-$ formulation.

In this work, we give what we judge to be an improved account of the preparation of RCS_3Cl (R = Ph, 1-naphthyl). We converted the chloride to the MF_6^- (M = As, Sb) salts by a metathesis reaction of $AgMF_6$ and RCS_3Cl in SO_2 solution. However, it is likely that these salts are better prepared via the readily accessible and anhydrous salts of RCS_2^-,[62] as implied by our preliminary results of the oxidation of $Zn(PhCS_2)$ by AsF_5. The soluble MF_6^- salts are more readily structurally characterized than the less soluble chloride precursors. The ionic formulation and structures of the MF_6^- salts of RCS_3^+ (R = Ph, 1-naphthyl) were established by vibrational spectroscopy, multinuclear NMR, and in addition a preliminary X-ray structure of **1**SbF_6, which confirmed atomic connectivity, and supported by a good fit of all the experimental data by hybrid HF-DFT (MPW1PW91) calculations. The structure of $PhCS_3Cl$ was inferred as largely ionic as the chloride and SbF_6^- salts were interconvertible via metathesis reactions. The vibrational spectra were similar to but not identical to those of **1** in the **1**MF_6 salts and consistent with an ionic formulation with substantial $S^{\delta+}\cdots Cl^-$ interaction. The mass spectra of $PhCS_3Cl$ implied a covalent structure in the gas phase.

The structural data for **1** and **3** as well as the calculated structures lead us to infer that the $-CS_3^+$ ring is strained (Figure 2), having the smallest SSS angle so far reported as far as we are aware. Positive charge is largely located on the sulfur atoms as expected, but there is also some positive charge delocalization into the phenyl ring which likely stabilizes the cation. The bond distances imply that the π bonding in the ring is largely restricted to the C−S bonds. However, a preliminary MO analysis suggests that the ring has some aromatic character. A complete description of the nature of the bonding in the ring, estimations of ring strain, etc. awaits a more extensive theoretical analysis.

Acknowledgment. We thank Mr. Gilles Vautour for obtaining mass spectra, Dr. Larry Calhoun for aid with NMR spectroscopy, Dr. Joel F. Liebman for discussions, Dr. Dennis Connor for the X-ray powder diffraction measurements, Dr. Carsten Knapp for proofreading the manuscript, NSERC (Canada) for a discovery grant (J.P.), and the Province of New Brunswick for a Women's Doctoral Fellowship (M.F.).

Supporting Information Available: Tables and figures included in the Supporting Information are given labels precedent with "S-". They include the following: S-Table 1, Preparative data for $PhCS_3Cl$; S-Table 2, Preparative data for **1**SbF_6; S-Table 3, Vibrational spectral data for some chlorides and their corresponding AsF_6^-, SbF_6^-, and $SbCl_6^-$ salts; S-Table 4, Mass spectral data for the recovered **14**Cl from the reaction of $C_{10}H_7CS_2H$ and SCl_2; S-Table 5, Tentative assignment of the vibrational spectra of **14**Cl and **14**SbF_6; S-Table 6, A comparison of the observed vibrational data for **1** in **1**SbF_6 with the calculated (MPW1PW91) values using 3-21G* and 6-31G* basis sets with C_{2v} geometry or without symmetry restriction; S-Table 7, A comparison of the observed vibrational data for **14** in **14**SbF_6 with the calculated (MPW1PW91) values using 3-21G* and 6-31G* basis sets; S-Table 8, P_z orbital coefficients for C1, C2, S3, S4, and S5 of the occupied π MOs of **1** shown in Figure 4; S-Figure 1, Reaction vessels; S-Figure 2, FT-Raman and FT-IR spectra of $PhCS_3Cl$; S-Figure 3, FT-Raman and FT-IR spectra of **1**SbF_6; S-Figure 4, ^1H NMR spectrum of $C_{10}H_7CS_2H$ in $CDCl_3$; S-Figure 5, In situ ^1H NMR spectrum of the products of the reaction of $PhCS_3Cl$ (produced from NBu_4Cl/**1**SbF_6 reaction) and $AgSbF_6$ in liquid SO_2 after 15 min; S-Figure 6, FT-Raman spectrum of $PhCS_3Cl$; S-Figure 7, FT-Raman and FT-IR spectra of **14**Cl; S-Figure 8, FT-Raman and FT-IR spectra of **14**SbF_6; S-Figure 9, Comparison of the FT-Raman of **14**SbF_6 and **14**Cl in the region of 2000−50 cm^{-1}; S-Figure 10, In situ ^1H NMR studies of **1**SbF_6 in liquid SO_2 at room temperature; S-Figure 11, In situ ^{13}C NMR studies of **1**SbF_6 in liquid SO_2; S-Figure 12, In situ ^1H and ^{13}C NMR studies of the purified **14**SbF_6 in liquid SO_2 at room temperature as a function of time; S-Figure 13, In situ ^1H, ^{19}F, and ^{13}C NMR spectra of the recovered **14**SbF_6 (from the reaction of **14**Cl and $AgSbF_6$) in liquid SO_2 at room temperature as a function of time, showing the presence of impurities; S-Figure 14, Depictions of the calculated vibrational modes of **1** (MPW1PW91/6-31G*); S-Figure 15, Depictions of the calculated vibrational modes of **14**; S-Figure 16, ^1H NMR spectrum of the products of the reaction of $Zn(PhCS_2)_2$ and AsF_5 in liquid SO_2 after 1 day;

(62) Kato, S.; Yamada, S.; Goto, H.; Terashima, K.; Mizuta, M.; Katada, T. *Z. Naturforsch.* **1980**, *35b*, 458.
(63) Huheey, J. E.; Keiter, E. A.; Keiter, R. L. *Inorganic Chemistry*, 4th ed.; HarperCollins College: New York, 1993.
(64) Brese, N. E.; O'Keeffe, M. *Acta Crystallogr., Sect. B* **1991**, *47*, 192−197.
(65) Small, R. W. H.; Banister, A. J.; Hauptman, Z. V. *J. Chem. Soc., Dalton Trans.* **1984**, 1377−1381.
(66) Pauling, L. *The Nature of the Chemical Bond*, 3rd ed.; Cornell University Press: Ithaca, NY, 1960.

S-Figure 17, HOMO-2 and HOMO-3 molecular orbitals (isosurface drawn at 0.01 au) of HCS_3^+ (MPW1PW91/6-311+G(d)) and S_4^{2+} (B3PW91/6-311+G(d)); S-Figure 18, In situ ^{19}F and ^1H NMR spectra of **1**SbF_6 in liquid SO_2 after 7 days at room temperature; S-Figure 19, Depictions of the calculated vibrational modes of $PhCS_2^-$ (MPW1PW91/6-31G*); Preparation of crystals of **1**SbF_6; Purification of **1**SbF_6; Attempted synthesis of **2**$(AsF_6)_2$ by the reaction of $Zn(PhCS_2)_2$ and AsF_5 leading to **1**AsF_6; Comparison of the synthesis of **1**AsF_6 by the oxidization of $Zn(PhCS_2)_2$ by AsF_5 with the synthesis of **1**SbF_6 by the reaction of $AgSbF_6$ with $PhCS_3Cl$; Vibrational spectra of $PhCS_3Cl$ and structural implications; Assignments of ^1H and ^{13}C chemical shifts of **14**SbF_6. This material is available free of charge via the Internet at http://pubs.acs.org.

IC049759S